JOURNAL OF STRESS ANALYSIS

Journal of Stress Analysis
Vol. 6, No. 1, Spring − Summer 2021, 1-12

Bu-Ali Sina University

ORIGINAL RESEARCH PAPER

Effect of the Bolt Layout and Distance on Strength of the Composite Joints

N. Habibi*, **S.H. Mousavi**

Mechanical Engineering Department, Faculty of Engineering, University of Kurdistan, Sanandaj, Iran.

Article info

Article history:
Received 16 April 2021
Received in revised form
08 July 2021
Accepted 27 July 2021

Keywords:
Bolted joint
Composite
Epoxy-glass
Numerical analysis
Tensile test

Abstract

Considering the importance of composite connections, this study evaluated two experimental and numerical methods for bolted joints of epoxy-glass composite plates. Then, using an artificial neural network, a model was defined between experimental and numerical results. The results of this study showed that the maximum force tolerated by bolted joints was various at several distances and its maximum value was tolerated by the connection at 4cm equal to 5332 and 7093N, for two specimens. Comparison of numerical and experimental results of Von-Mises stress for distances of 2, 3, and 4cm was done. The Von-Mises stress for these distances was 313.59, 217.57, and 177.71MPa, respectively. In this research, the connection of epoxy-glass plates using M6-bolt was studied, and by increasing the coverage of two composite plates, the Von-Mises stress in the connection was raised. Concerning the determination of the stress measuring path, from the internal edge of the critical notch to the end of the defined range with a smaller mesh, the Von-Mises stress was extracted, which in distance equal to 3cm with the vertical arrangement, maximum stress was equal to 513MPa. The minimum stored energy of the numerical method in the connection was related to the bolted joint with a two-bolt in the vertical position.

Nomenclature

d_{bolt}	The bolt diameter	t	Thickness of plates
d_{hole}	The hole diameter	$\sigma_{von.max}$	Maximum stress of Von-Mises
d	The distance of bolt to connection edge	ν	The Poisson's ratio
P	The force applied to the connection	T	The tightening torque
G_{bolt}	Shear modulus of bolt	G	Stored energy
W/D	The ratio of the joint width to the hole diameter	e/D	The ratio of the edge distance to the bolt hole diameter
$G_{\min}$	Minimum stored energy		

1. Introduction

Nowadays, composites due to lightness and high strength are used in various types of engineering structures, including spacecraft, airplanes, cars, boats, railways, bridges, and buildings in a wide range of materials. These structures are usually produced from joining members to transfer and sustain the applied forces. Although in recent years, composite construc-

*Corresponding author: N. Habibi (Assistant Professor)
E-mail address: n.habibi@uok.ac.ir
http://dx.doi.org/10.22084/jrstan.2021.23733.1173
ISSN: 2588-2597

tion techniques have made it possible to construct large structures with complex shapes and geometry, in many cases, to achieve the desired structure, it is necessary to connect the parts of the composite plates. There are two main methods for these connections: adhesive joints and mechanical connections. Mechanical joints are usually used in places where relatively thick structures are used, or to control and maintain the separation of parts. These connections will eventually suffer fatigue and ultimately failure [1]. In one of the oldest studies [2], the effect of stacking sequence on the pin-bearing strength in glass fiber reinforced plastics were studied. Moreover, damage tolerance of laminated composites containing an open hole under compressive loadings was investigated [3]. Furthermore, stress and failure analysis of mechanically bolted joints in composite laminates [4] and Finite Element (FE) modeling of damage accumulation bolted composite joints subjected to incremental tensile loading [5] were studied and a 3D progressive damage model was developed to simulate the damage accumulation of bolted single-lap composite joints under in-plane tensile loading [6]. Okutan [7] investigated stress and failure analysis of laminated composite pinned joints. Sun and colleagues, [8, 9] performed extensive experiments to characterize the material response due to bearing failure in composite bolted joints with/without lateral clamp-up supports.

McCarthy et al. [10] studied the effects of bolt-hole clearance on the stiffness and strength of composite bolted joints. Kradinov and colleagues [11] evaluated an analytical method to account for the variation of stresses in the thickness direction. McCarthy and co-workers, [12-14] used practical experiments and the 3D FE method for studying the effect of bolt hole tolerance and friction on single-bolt and single-shear composite joints and they developed a computational approach for modeling nonlinear elastic behavior in multi-bolts composite joints. Song et al. [15] studied the bearing strength of a single-edge riveted carbon/epoxy composite connection under temperature. Panigrahi and Pradhan [16] studied the growth of adhesion failure and delamination-induced damage in the laminated FRP composite joints. Tserpes et al. [17] evaluated the strength prediction of bolted joints in graphite/epoxy composite laminates. In addition, failure behavior, and stress distribution around the hole in laminated composite joints were investigated [18, 19]. Kapti et al. [20] evaluated the effect of preload torque and moisture on bearing strength and fracture modes in the pinned and bolted joints of epoxy carbon plates under tensile force. The effect of clamping force and friction coefficient on stress intensity factors (SIFs) of cracked lapped joints was researched [21].

The experiment and FE studies were deployed to determine the pin-load distribution of multiple countersunk bolted single-lap joints [22]. In the experimental studies, the pin-load fractions were evaluated indirectly by the lap-sheet surface strains collected from a few rows of strain gages. In the other work, [23] lapped bolted joints were modeled numerically to study the effect of a crack on the ultimate response of the joint. Due to the complexity of composite materials, numerical methods were generally utilized in their analysis and design. Commercial FE codes, such as ANSYS and ABAQUS, allow the implementation of user subroutines in the program [24]. FE and artificial neural networks (ANN) methods are widely used in such tasks to reduce time, money, and efforts consumed in laboratory experiments. 3D elastic-plastic FE analysis was adopted to simulate the failure stages of double lap joint [25]. The effect of the presence of crack located at the fastener hole surface of bolted metallic and polymeric joints on their ultimate strength and converting their failure mode has been studied [26].

In the research of Aleksandrova, [27] two geometrical models of bolted joints and pressurized containers were suggested. In the other new research, [28] the effect of clamping force on the bolted double-lap joints has been investigated. Ataei and co-workers, [29] investigated flush end-plate beam-to-column composite joints with precast slabs and deconstructable bolted shear connectors.

In the other paper, [30] the analysis of a steel beam-to-column bolted end-plate connection under cyclic loading was studied. Zhao et al. [31] proposed a probabilistic model including random geometrical dimensions, angles of fibers direction, and material properties to predict the eventual failure of a two-edge single-bolt connection [32]. Konkong and Phuvoravan [33] studied the effect of geometric variables on the bolt load distributions of a cold-formed steel bolt connection. El-Sisi and colleagues, [34] using a 3D FE model analyzed the single and double lapped bolted composite plates. Different bolt layouts, including the staggered arrangement, were examined and combined with other parameters such as the number of bolts, clamping force, and friction coefficient. Mechanical properties of laminated bamboo and the behavior of bolted joints using laminated bamboo and steel plates were studied [35]. In the research by Abd-Elhady et al. [36] the effects of W/D and T, with a constant value of e/D, were evaluated experimentally and concluded that prediction of failure stages of double lap bolted joints is an important design task.

A great deal of research was done on mechanical joints in composite materials, considering various parameters such as materials used and geometric properties with one or a combination of fracture criteria, so that fracture loading from joint strength by performing tests, calculations, and numerical method predicted. In the mentioned studies, the effect of bolt distance from the composite joint edge (d) with bolt layout has not been evaluated, and mostly, analyses were done with the help of computational and numerical methods to reduce the time and cost.

In this study, the effect of bolt distance from the bolted joint edge was evaluated using experimental and numerical methods. In addition, the optimal distance using ANN was determined and stress distribution for the two-bolt layout (horizontal and vertical) was obtained. The experimental analysis of the connections in a large structure is a time-consuming and costly task. It is important to use the appropriate criteria to find the most critical mechanical connection in the accurate numerical modeling of the connections of large structures [37]. Due to the mechanical properties of composite materials, it is not easy to use conventional methods (welding) to connect them to other materials. There are several methods for connecting composites, such as bolted joints. In this research, we have examined single-lap composite bolted joints. The reason for using this bolt (M6) is its proper diameter for thin plates. Epoxy glass composites compared with metals due to their high mechanical properties in terms of weight and high strength to corrosion, are widely used in various industries including aerospace and automotive, and according to studies on this type of joint, it is abundantly used in car bodies.

In the connection to avoid the use of large diameter bolts, it is preferable to use two-bolt with a smaller diameter so that the holes in the composite body have a smaller diameter and do not harm the strength of the composite joint, therefore, two-bolt for connection was investigated. But, two-bolted joints with two different layouts at a fixed distance from each other and the effect of the distance between the two bolts have not been studied, which can be investigated in future researches. Of course, the selection of two-bolt (horizontal and vertical positions) to examine the concentration of tension in the two states next to each other and a row has been examined. In this work, composite plates of the bolted joint under tensile test and numerical method using ABAQUS software were studied. Because of the hole in the composite plate, the stress around the hole is high and the composite may fail. Composite behavior analysis at the connection is important after the damage begins and in most connections require a 3D damage analysis.

2. Experimental Section

For the production of composite plates, the EPOLAM epoxy resin and its hardening were used (Axson France Company). The E-glass woven fabric cloth (Colan Australia) was also used with a surface weight of 195g/m^2 and a net thickness of 0.28mm. All composite plates were cured together at a temperature of 50°C for 15 hours. The selection of bolt diameter depends on the size of the plates and loading conditions.

Nowadays, Glass-epoxy composite has a significant position rather than metals due to high mechanical properties compared with low weight as well as high corrosion resistance in various industries such as aerospace, automobile, and defense. According to the performed studies, this bolted joint in the chassis of the vehicle is widely used [17]. Dimensions of composite plates were as the following: length and width of plates were 10 and 3cm respectively. Dimensions of the samples were selected following the limitations of the test machine jaw (Model of tensile testing: SANTAM-AST150). In these experiments, the M6 bolt was used. Since in the bolted joint, $d = 2, 3$, and 4cm were studied, and two samples were tested for any distance, therefore, the number of tested joints was 6 samples. Fig. 1a illustrates loading on composite connection. The specifications of the bolt used were as follows: Class 5.6, nominal diameter and root diameter were 5mm, 4.773mm, area of the cross-section was 17.733mm^2 and maximum force was 8524N. Moreover, the properties of epoxy glass are as follows: yield stress was 65-70MPa, tensile strength was 70-75MPa and elasticity modulus was 12-14GPa.

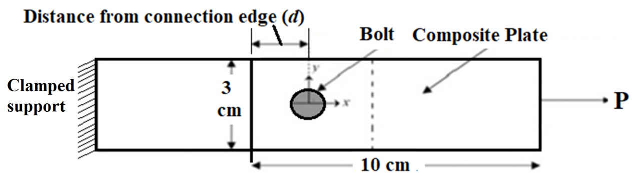

(a)

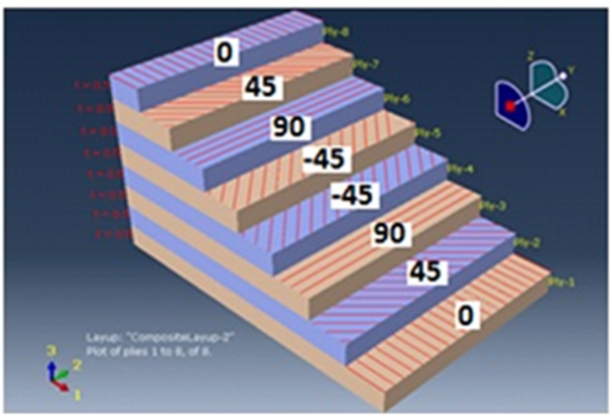

(b)

Fig. 1. Schematic of a) Loading for composite bolted joint, b) Composite plate with fiber alignment angle [15].

In this research, eight-layered composite plates with symmetrical layers and angles were used (Fig. 1b) [15].

In the present study, standard ASTM D5961/D5961M-05 was used to prepare and perform experiments [38]. Composite plates were connected by bolts and specimens under tensile loading. On the other hand, the force-displacement curves of the test specimens were recorded by the operating system connected to the tensile test apparatus. In this process, it was observed that the bolt in the specimens caused bearing damage and rupture of the fibers. The bolt also began to bend due to the high strength of the composite plates during the loading phase. Finally, the bolt fractured due to the low strength of the bolts compared with the strength of the composite plates under the maximum applied load. Applied load to composite bolted joint in Fig. 2a is demonstrated.

(a)

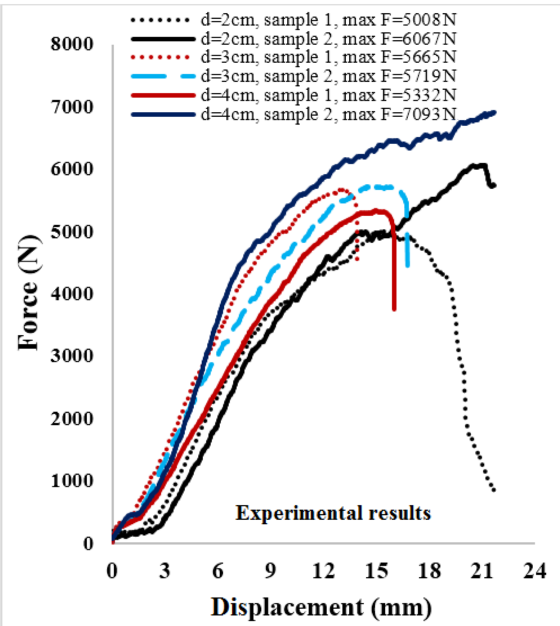

(b)

Fig. 2. a) The composite bolted joint with test apparatus, b) Experimental force-displacement curve versus d.

In Fig. 2b, the experimental results with different distances and repetitions are demonstrated. In the first samples (1, 2), $d = 2$cm, these samples stretched from zero to 3mm due to the insignificant initial clearance of bolt and composite plate hole. With modest stress, after this step, and completely tightening the composite plates and bolt, the force increased to 5, 6kN for two specimens, and during this increase, the displacement continued to exceed 16 and 23mm in 2 samples. In two specimens, before the composite complete damage, the bolt of the composite joint bent, and the composite plate fell into disrepair and somewhat ruptured.

For the second specimens $(3, 4)$, $d = 3$cm, in addition, the force increased to 5.4 and 5.5kN, the displacement continued to exceed 15 and 17mm, and before the composite complete damage, the bolt of composite joint fractured, and the composite plate fell into disrepair and somewhat ruptured. The composite plate was crushed but less ruptured than the previous two because, before the change in the length of the composite plates to increase the rupture, the bolt of the joint cut, and the test was stopped.

In the third samples $(5, 6)$, $d = 4$cm, the force increased to 5.2 and 7kN, and the displacement continued to exceed 17 and 25mm. In these two experiments, like the second specimens (3,4), the bolt of composite joint failed, also, transverse and longitudinal cracks were observed in the connection hole. Experimental results versus d are shown in Fig. 2. In addition, the composite plate was crushed. Furthermore, the maximum tolerated force in the bolted joint occurred at $d = 4$cm and the tensile strength connection increased with increasing d.

3. Numerical Section

Tensile tests of glass-epoxy composite bolted joint using ABAQUS software were simulated in states with $d = 2, 3$, and 4cm for determining optimal arrangement in two layout bolts (vertical and horizontal positions). After the analysis, the optimal layout was selected. It should be noted that the M6 bolt was used. Fig. 3a shows a bolted joint model in software. Before the final analysis and numerical results extraction, the meshing independence was evaluated. The numerical method of this modeling was done as nonlinear static analysis (solver). Moreover, the implicit solution method was selected. Because often in the static modeling, the FE solution is implicit. In this modeling, the solid element was considered for bolt and the bolt deformation in comparison to composite plates was small. Regarding the contact between the bolt and the nut, it is restricted to six degrees of freedom, the clearance isn't considered. The material behavioral model was considered as the two-line model.

3.1. Validation of Meshing and Results

To reduce the amount of simulation calculations time and the processing volume in the computer, a regional meshing technique was used that considers a circle with 12mm in diameter around the hole as the target area, because the greatest damage occurs in the hole domain. Figs. 3a and 3b show loading and meshing around the hole of the bolted joint.

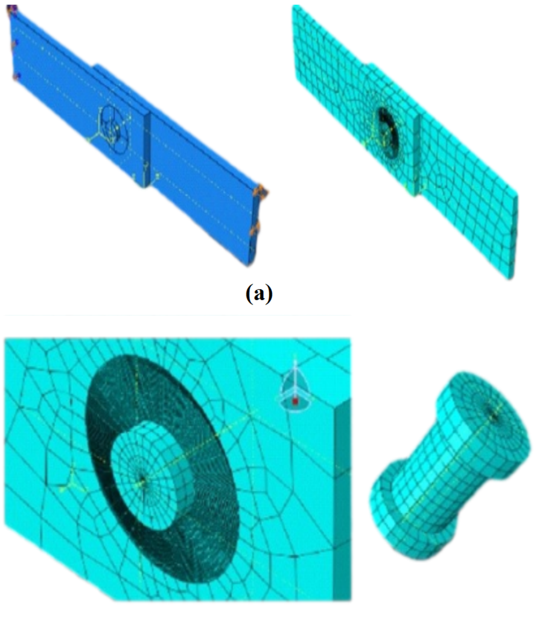

Fig. 3. Schematic of a) Loading, b) The meshing of the composite bolted connection, c) The meshing of bolt and notch.

Fig. 3c shows the bolt and composite plates in the connection area separately. To verify the mesh independence, $d = 2$cm in the software is considered. In this assessment, the amount of stress in a range around the hole was considered as the basis, and the meshing from 500 to 4000 elements changed around the hole.

The results of this change indicated that a reduction for the stress variations in the mesh range 2000 is up and as follow: 500(65), 1000(62), 1500(59), 2000(56.2), 2500(56), 3000(55), 3500(55), where the numbers in parentheses are σ_{von} (MPa). The calculation of the σ_{von} was determined around the notch (Fig. 4a), that extending from the inner edge of the notch to the end of the meshing area with a diameter of 12mm. According to the software simulations in Fig. 4a, at $d = 2$cm, the maximum stress related to the inner edge of the notch with $d = 0.22$mm ($\sigma_{von} = 252$MPa).

The σ_{von} in the notch range between 128 up to 252MPa is changed and decreases with the distance from the inner edge.

In addition, at $d = 2$cm, the σ_{von} in the notch range between 134 up to 443MPa is changed and the $\sigma_{von.max} = 443$MPa in the inner edge of the notch that its value decreases with the distance from the inner edge. At $d = 2$cm, the σ_{von} is not maximized at the edge of the notch, but at $d = 3$cm, the $\sigma_{von.max}$ occurs in the inner edge of the notch. In addition, at $d = 4$cm, the $\sigma_{von.max}$ related to the inner edge of the notch with $d = 0.50$mm ($\sigma_{von} = 325$MPa).

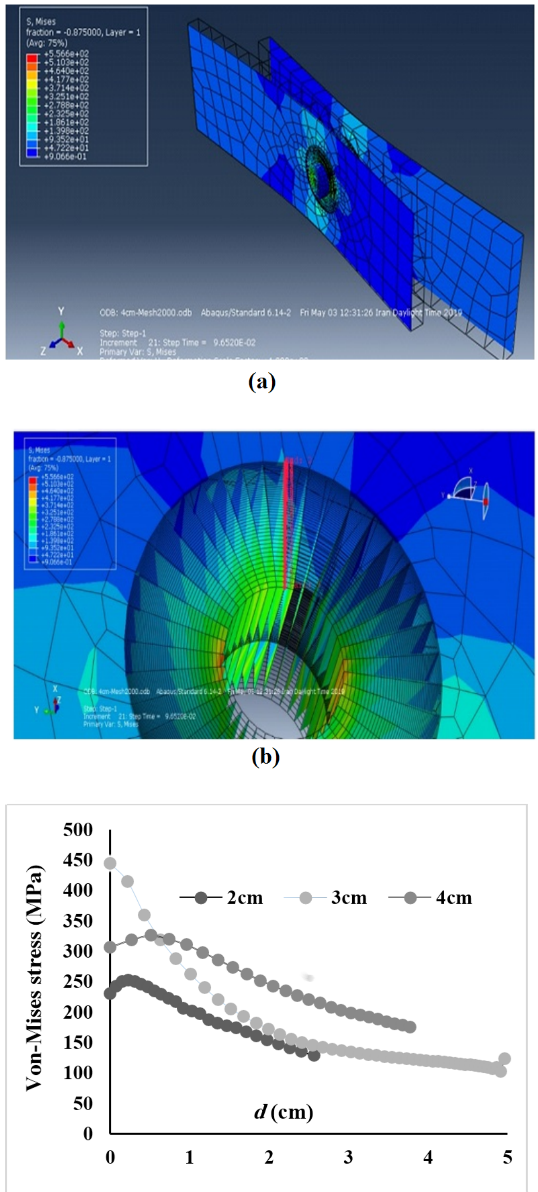

Fig. 4. a) The Numerical value of σ_{von} obtained in the ABAQUS software, b) Path for determinate σ_{von} around notch ($d = 4$cm) and c) σ_{von} in terms of d (numerical results).

The σ_{von} occurs in the notch range and its value between 200 up to 325MPa is changed. Path for determinateσ_{von} around notch is illustrated in Fig. 4b. Moreover, the σ_{von} (Fig. 4c), around the notch, by increasing d show that the σ_{von} changes like experimental results, since in laboratory samples; with increasing in covering of the bearing regions, stresses around the notch increase. In the study of d with the σ_{von} in each distance, the distance between the internal edges of the notch, the σ_{von} decrease, these changes occur due to distance from the bearing stress region. Most displacements at the end of the plates occur that are connected to the support. The displacement contour of the composite bolted joint is shown in Fig. 5.

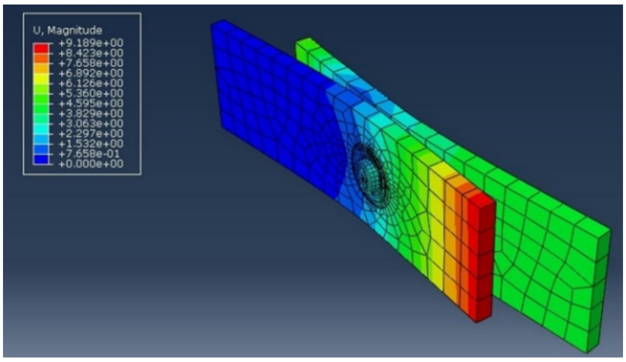

Fig. 5. Displacement contour of composite bolted joint ($d = 4$cm).

4. Artificial Neural Network Method

By extracting the results, their analysis for the composite behavior, using the ANN method (Fig. 6a) was evaluated, so that the model shows the behavior of the composite. This analysis is done based on Neuro Solution Software. The multi-layers Perceptron neural network is used with three inputs to determine the optimal mesh. For the mesh test, the learning method is used after error propagation for the network. Mean Squares Error for artificial neural network model are demonstrated in Fig. 6b. In the optimization section, an optimal overlapping distance of composite plates is determined using ANN, and this distance is calculated by examining the $\sigma_{von.max}$ around the hole at a distance of 0.1cm for the overlapping of the plates. This distance is 2.2cm with stress equal to 448MPa. In addition, d for two positions of bolts layout are 2.4 and 3.8cm that equivalent stresses are 381 and 556MPa, respectively.

In Table 1, the results of research in the optimal distance are illustrated for one-bolt, two-bolt (both layouts).

Table 1
The $\sigma_{\max}$ of ANN model.

σ_{max} (MPa), ANN			d (cm)	Test code
Number of bolts				
2	2	1		
Type of bolts layout				
2	1	0		
430	124	447(443*)	2.0	1
411	137	440	2.1	2
435	146	448	2.2	3
432	160	435	2.3	4
439	137	433	2.4	5
482	163	431	2.5	6
469	171	425	2.6	7
454	177	434	2.7	8
449	169	385	2.8	9
438	182	364	2.9	10
508	213	317(325*)	3.00	11
483	193	328	3.1	12
495	187	324	3.2	13
511	198	332	3.3	14
515	190	340	3.4	15
520	197	338	3.5	16
526	204	341	3.6	17
548	223	342	3.7	18
556	283	346	3.8	19
529	237	343	3.9	20
441	269	336(344*)	4.0	21
524	263	365	4.1	22
506	381	374	4.2	23
492	301	389	4.3	23
481	308	397	4.4	25
469	314	423	4.5	26

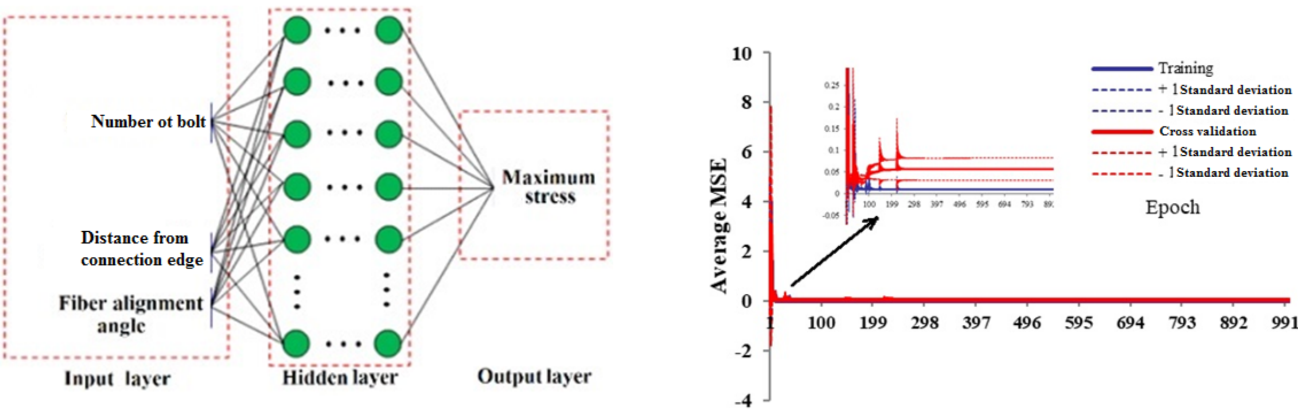

(a) (b)

Fig. 6. a) Tree diagram for ANN, b) Mean squares error for ANN model.

5. Discussion of Results

5.1. The Modes of Failure in the Bolted Joints

The main disadvantage of bolted joints is the formation of high-stress concentration zones at the locations of bolt holes, which might lead to a premature failure of the joint due to net-section, shear-out, or bearing failures, or their combinations. The modes of failure and their associated parameters which characterize the failure of composite bolted plates were presented in the previous studies [39-41].

The most important failure modes of composite bolted lapped joints. The net-tensile failure mode occurs due to the reduced connection width and due to the unidirectional fiber composite perpendicular to the applied load. The shear-out failure mode can happen because of the reduction in the end-distance and the unidirectional fiber composite parallel to the applied load.

The failure can be avoided in most cases by increasing the end-distance and use of the proper lay-up. A cleavage failure occurs because of a combination of insufficient joint width and edge distance [34].

As the bolt bends, the plies are loaded differently near the hole boundary based on their orientation and location. The plies close to the interface of adjacent laminates exhibit significant deformation. Bolts provide the primary means of connecting composite parts in the construction of aircraft and aerospace vehicles [11].

To simulate the progressive failure of the pinned joint in quasi-isotropic [0/45/-45/90]s glass fiber reinforced polymer composite laminates used in the pipeline, a 3D FE model is employed. Hashin failure criterion as a progressive damage model associated with the Virtual-Crack-Closing-Technique delamination model has been adopted to predict the failure due to fiber breakage and matrix cracking [42]. Most of the test specimens in the research of Khashaba et al. [40] failed in the following sequence: (a) delamination between the 0°, ±45° and 90° layers due to their different strains under the compressive bearing load, (b) net-tension failure mode for 90° layers, (c) shear-out failure modes for 0° layers, and (d) the final failure was nearly catastrophic due to the bearing failure of ±45° layers.

In Fig. 7, images of composite plates are illustrated after the tensile test, and the failure modes on the composite plates of the connection are as follows: shear-out, transverse splitting, and bearing, also failure and bending occurred in the threaded section of the bolts. Two types of screw failures were also observed: failure in bolt head and bolt thread failure.

5.2. Effect of Horizontal and Vertical Layouts

The results of the σ_{von} analysis are illustrated in Fig. 8a. As can be seen, at different distances, the downward trend of σ_{von} is evident from the inner edge of the hole toward the middle of the span (distance between two bolts). The σ_{von} before reaching the range between two bolts has incremental changes.

The σ_{von} for the bolted joints (two vertical bolts) according to Fig. 8b) are shown according to the butterfly shape of the stress concentration around the second hole and the path of stress distribution determine. The σ_{von} is downright before reaching the butterfly stress range. In the study of the effect of the layout, six cases versus d in both vertical and horizontal layouts were considered, and the results are shown in Fig. 8c. In horizontal positions of bolts, in three distances, the stress concentration between the two-hole occurred, but in the vertical position of bolts, the butterfly concentration stress created around the second hole. By determination of the path of calculation of stress from the internal edge of the hole is more critical to the end of the specified range with a fine mesh, the σ_{von} is calculated, and for $d = 3$cm with vertical layout has the maximum value ($\sigma_{von} = 513$MPa).

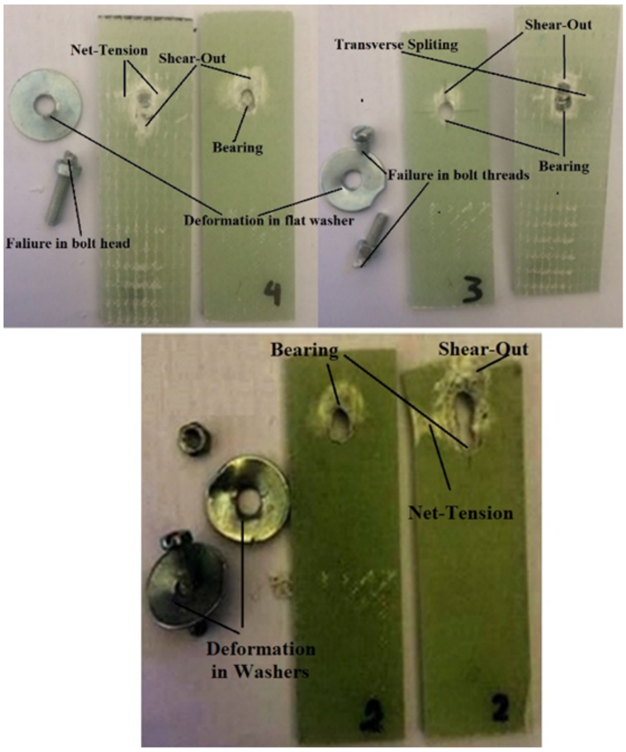

Fig. 7. Failure modes in composite bolted joints.

Fig. 8d illustrates the force-displacement curve for numerical analysis. According to $d = 4$cm results, it has the maximum force of 7290N. The displacement of the composite plate is measured relative to a fixed reference and ABAQUS software automatically measures this displacement.

5.3. ANN Method

According to Figs. 2b and 8d, the percentage of the difference between the maximum force in the experimental and numerical methods for different distances is observed that the min and max errors are about 10% and 20%, respectively.

According to the model results in Fig. 9, the calculated ANN and the numerical maximum stresses show that adaptation is very good. In addition, experimental and numerical methods are costly and time-consuming to extract results, therefore, the new distances are predicted by the ANN suggest. Using Excel software, curves with the lowest error were passed from the sixth degree (sixth-order polynomial) to the ANN data (two-bolt layout, Table 1, Fig. 10b), and the equations of $\sigma_{\max}$ (MPa) for two different layouts are as follows:

Two-bolt and two-layout

$$\sigma_{max} = 0.00005d^6 - 0.0095d^5 + 0.7346d^4 - 29.657d^3 + 661.54d^2 - 7730.1d + 37378$$

One-bolt and one-layout

$$\sigma_{max} = 0.00007d^6 - 0.0131d^5 + 1.0207d^4 - 41.574d^3 + 930.75d^2 - 10859d + 52063$$

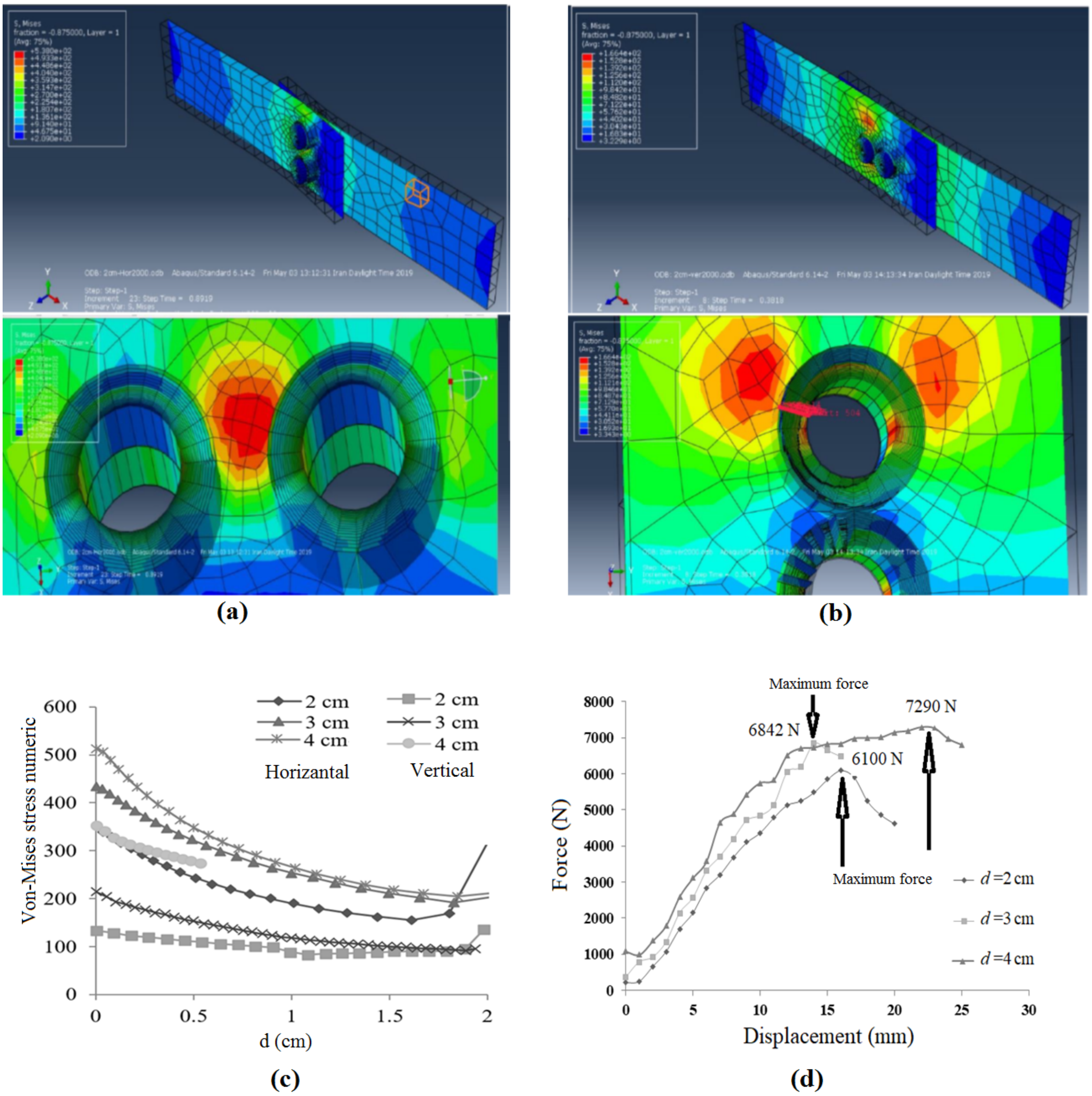

Fig. 8. The σ_{von} for horizontal layout of two-bolt ($d = 2$cm), a) Horizontal layout, b) Vertical layout, and c) The σ_{von} in surround notch versus d, and d) Force-displacement curves, (numerical results).

To derive a more accurate function, a five-order polynomial was covered in three regions, the equations of stress (one-bolt and one-layout) are as follows:

$$\sigma_{max} = -0.0994d^5 + 11.713d^4 - 550.51d^3 + 12894d^2 - 150517d + 700963$$

$$20 \le d \le 28 \cdot R^2 = 0.9618$$

$$\sigma_{max} = -0.0255d^5 + 4.4189d^4 - 305.91d^3 + 10567d^2 - 182111d + 10^6$$

$$29 \le d \le 30 \cdot R^2 = 0.909$$

$$\sigma_{max} = 0.6417d^5 - 136.37d^4 + 11590d^3 - 492325d^2 + 10^7d - 9 \times 10^7$$

$$40 \le d \le 45 \cdot R^2 = 1.0$$

Additionally, the five- and six-order polynomials were fit in three regions, the equations of stress (two-bolt and two-layout) are as follows:

$$\sigma_{max} = 0.0771d^6 - 11.046d^5 + 657.37d^4 - 20809d^3 + 369532d^2 - 3 \times 10^6d + 10^7$$

$$20 \le d \le 28 \cdot R^2 = 0.9038$$

$$\sigma_{max} = -0.0236d^6 + 4.8195d^5 - 410.02d^4 + 18571d^3 - 472305d^2 + 6 \times 10^6d - 4 \times 10^7$$

$$29 \le d \le 39 \cdot R^2 = 0.9690$$

$$\sigma_{max} = 0.8583d^5 - 184.67d^4 + 15887d^3 - 683213d^2 + 10^7d - 10^8$$

$$40 \le d \le 45 \cdot R^2 = 1.0$$

where d is the distance from notch edge (mm).

In Fig. 10a, numerical and experimental bearing stresses versus d are shown.

According to Table 1, for different distances from the edge equal to 2, 3, and 4cm, the maximum stresses for one bolt are 443, 325, and 344MPa, respectively. According to the neural network method, these amounts of stresses are equal to 447, 317, and 336MPa. If the stress resulting from the neural network method is used as the basis for the stress ratio, this ratio is 0.99, 0.125, and 1.024 for $d = 2, 3$, and 4cm, respectively. This ratio shows that the neural network and the numerical methods have provided close results and due to the compatibility of experimental and numerical (simulation) results, the artificial neural network method can be used as an efficient and capable method to solve problems of engineering.

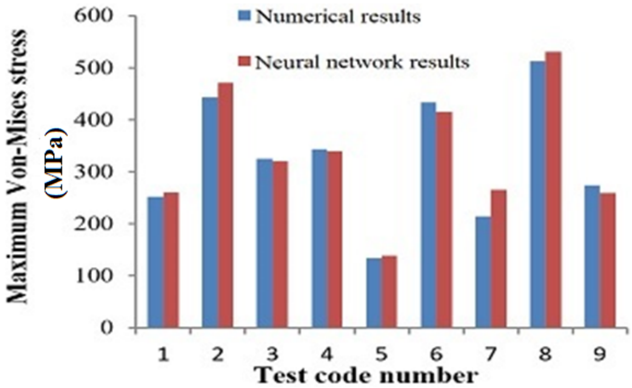

Fig. 9. The $\sigma_{von,max}$ using numerical and ANN methods.

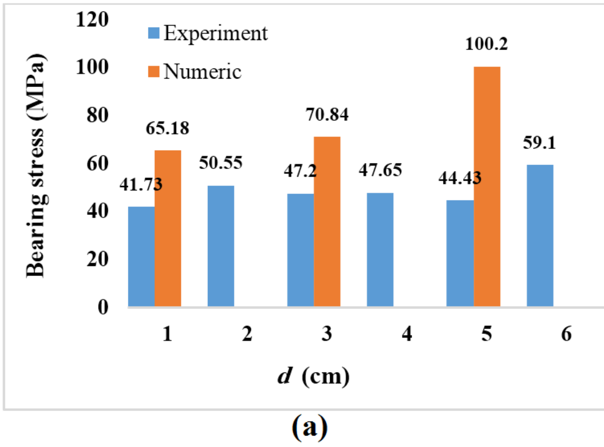

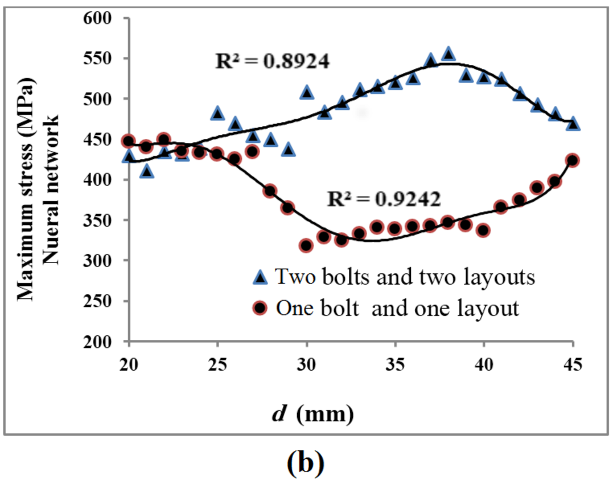

Fig. 10. a) Numerical and experimental bearing stresses, b) Passing curves with proper accuracy (ANN data).

Table 2
The **G** in the composite bolted joints.

d(cm)	No. sample	**G**(Nm)			
		Experiment	Numeric		Numeric
			1-bolt	Horizontal 2-bolts	Vertical 2-bolts
2	1	51.02	23.5	34.9	13.9
	2	100.54			
3	1	53.85	44.3	43.4	21.5
	2	70.13			
4	1	76.81	78.77	51.3	35
	2	170.62			

5.4. The Stored Energy (G) in the Bolted Joints

The area below the force diagram in terms of displacement of composite bolted joints to failure is equal to the **G** in the connection and is considered of great importance in the design of these joints. In the newest research, Jazib Hassan et al. [43] studied the **G** capability of composite bolted joints undergoing extended bearing failure. Moreover, Carcaterra and Negamile [44] evaluated **G** in bolted joint components and the development of a geometry selection design tool for Belleville washers. **G** in these specimens (experiment and numeric) are demonstrated in Table 2.

According to this table, the lowest stored energy ($\mathbf{G}_{min}$) in the connection is related to the bolted joint with two-bolt in the vertical position (numerical method), and with increasing d, the value of **G** increases. Therefore, in designing this type of connection, the horizontal position of bolts is given priority over vertical ones.

6. Conclusions

In the present research, the composite plates bolted joints were tested using the tensile test apparatus and simulated in the ABAQUS software. Furthermore, for the determination of optimal d, the ANN method was used. The results of the present study are summarized as follows. The maximum forces tolerated by bolted joint were different at several distances. At $d = 2$cm, the forces 5008 and 6067N are tolerated by connection, so the bolt bends and tear occur on the composite plates. In addition, at $d = 3$cm, the forces 5665 and 5719N are tolerated by joint, and in that distance, before the complete damage to the composite plates, the bolt was cut, in which the composite plates were crushed, but less prone than the specimens with $d = 2$cm. However, the plates were less ruptured than the samples at $d = 2$cm.

For $d = 4$cm, the forces of 5332 and 7093N are tolerated by bolted joints, and the behavior of the composite plates and the bolted joint in terms of fracture and tearing is like $d = 3$cm. In composite joints, none of the composite plates completely tore, but the plates that attached to the moving jaw of the test apparatus were further damaged. According to numerical and experimental bearing stresses in terms of d, the σ_{von} for $d = 2, 3$ and 4cm are 313.59, 217.57 and 177.71MPa, respectively.

In the study of the effect of the bolts' arrangement, several locations were studied at $d = 2, 3,$ and 4cm for vertical and horizontal alignments. In horizontal positions of the bolts, in three distances, stress concentration occurred between the two notches, but in the vertical position of bolts, the butterfly stress concentration occurred around the second notch. About the determination of the stress calculation path, from the internal edge of the critical notch to the end of the defined range with a smaller mesh, the σ_{von} was calculated, which in $d = 3$cm with the vertical layout, $\sigma_{max} = 513$MPa.

$\mathbf{G}_{\min}$ is related to the bolted joint with a two-bolt in the vertical position (numerical method), and with increasing d, this amount of energy increases. The percentage difference between the maximum force in the experimental and numerical methods for different d showed that the min and max error is about 10% and 20% respectively. According to the maximum stress equations in terms of d obtained from the ANN method, with proper accuracy, the amount of maximum stress for other distances in both horizontal and vertical positions of the bolts can be calculated.

Acknowledgment

Thanks, and appreciation to Iran Composite Company for the preparation of test samples and from the Technical Laboratory of Soil Mechanics of Elam Province (Mechanics of Materials Section) to perform composite bolted joints tensile tests and Mr. Mousavi, who did a lot of study in the experimental and numerical sections.

Declaration of Conflicting Interests

The authors declare that there is no conflict of interest regarding the publication of this paper.

References

[1] T. Sinmazcelik, E. Avcu, M.Ö. Bora, O. Coban, A Review: Fiber metal laminates, background, bonding types and applied test methods, Mater. Des., 32(7) (2011) 3671-3685.

[2] W.J. Quinn, F.L. Mathews, The effect of stacking sequence on the pin-bearing strength in glass fiber reinforced plastics, J. Compos. Mater., 11(2) (1977) 139-145.

[3] C. Fu-Kuo, B.L. Larry, Damage tolerance of laminated composites containing an open hole and subjected to compressive loadings: Part I-analysis, J. Compos. Mater., 25(1) (1991) 2-43.

[4] M.L. Dano, G. Gendron, A. Picard, Stress and failure analysis of mechanically fastened joints in composite laminates, Compos. Struct., 50(3) (2000) 287-296.

[5] Th. Kermanidis, G. Labeas, K.I. Tserpes, Sp. Pantelakis, Finite element modeling of damage accumulation bolted composite joints under incremental tensile loading, European Congress on Computational Methods in Applied Sciences and Engineering, Barcelona, Spain,Barcelona, 11-14 September (2000).

[6] J. Hanauska, V. Kradinov, E. Madenci, A composite double-lap joint with staggered bolts: an experimental and analytical investigation, Compos. Struct., 54(1) (2001) 3-15.

[7] B. Okuta, Stress and failure analysis of laminated composite pinned joints, Ph.D. Thesis, School of Natural and Applied Sciences, Dokuz Eylul University, (2001).

[8] H.T. Sun, F.K. Chang, X, Qing, The response of composite joints with bolt clamping loads, Part I: Model development, J. Compos. Mater., 36(1) (2002) 47-67.

[9] H.T. Sun, F.K. Chang, X. Qing, The response of composite joints with bolt-clamping loads, Part II: Model verification, J. Compos. Mater., 36(1) (2002) 69-92.

[10] M.A. McCarthy, V.P. Lawlor, W.F. Stanley, C.T. McCarthy, Bolt-hole clearance effects and strength Criteria in single-bolt, single-lap, composite bolted joints, Compos. Sci. Technol., 62(10-11) (2002) 1415-1431.

[11] V. Kradinov, E. Madenci, D.R. Ambur, Combined in-plane and through-the thickness analysis for failure prediction of bolted composite joints, 45th AIAA/ASME/ASCE/AHS/ASC Structures, Structural Dynamics & Materials Conference, Palm Springs, California, 19-22April (2004).

[12] C.T. McCarthy, M.A. McCarthy, V.P. Lawlor, Progressive damage analysis of multi-bolt composite joints with variable bolt-hole clearances, J. Compos. B., 36(4) (2005) 290-305.

[13] M.A. McCarthy, C.T. McCarthy, G.S. Padhi, A simple method for determining the effects of bolt-hole clearance on load distribution in single-column multi-bolt composite joints, Compos. Struct., 73(1) (2005) 78-87.

[14] M.A. McCarthy, C.T. McCarthy, V.P. Lawlor, W.F. Stanley, Three-dimensional finite element analysis of single-bolt, single-lap composite bolted joints, part I: model development and validation, Compos. Struct., 71(2) (2005) 140-158.

[15] M.H. Song, J.H. Kweon, S.K. Kim, C. Kim, T.J. Lee, S.M. Choi, M.S. Seong, An experimental study on the failure of carbon/epoxy single lap riveted joints after thermal exposure, Compos. Struct., 86 (1-3) (2008) 125-134.

[16] S.K. Panigrahi, B. Pradhan, Onset and growth of adhesion failure and delamination induced damages in the double lap joint of laminated FRP composites, Compos. Struct., 85(4) (2009) 326-336.

[17] K.I. Tserpes, G. Labeas, P. Papanikosb, Th. Kermanidis, Strength prediction of bolted joints in graphite/epoxy composite laminates, Compos. B., 33(7) (2002) 521-529.

[18] R. Karakuzu, C.R. Caliskan, M. Aktas, B.M. Icten, Failure behavior of laminated composite plates with two serial pin-loaded holes, Compos. Struct., 82(2) (2008) 225-234.

[19] V. Yavari, I. Rajabi, F. Daneshvar, M.H. Kadivar, On the stress distribution around the hole in mechanically fastened Joints, Mech. Res. Commun., 36(3) (2009) 373-380.

[20] S. Kapti, O. Sayman, M. Ozen, S. Benli, Experimental and numerical failure analysis of carbon/epoxy laminated composite joints under different conditions, Mater. Des., 31(10) (2010) 4933-4942.

[21] H.E.M. Sallam, A.E.A. El-Sisi, E.B. Matar, O.M. El-Hussieny, Effect of clamping force and friction coefficient on stress intensity factor of cracked lapped joints, Eng. Fail. Anal., 18(6) (2011) 1550-1558.

[22] X.D. Liu, Y.Z. Li, Z.H. Yao, H. Shu, Study on the pin-load distribution of multiple-bolted composite to metal joints, Key Eng. Mater., 525-526 (2012) 285-288.

[23] A.E.A. El-Sisi, H.A. Salim, O. M. El-Hussieny, H.E.M. Sallam, Behaviors of a cracked lapped joint under mixed-mode loading, Eng. Fail. Anal., 36 (2014) 134-146.

[24] A.E.A. El-Sisi, H.M. El-Emam, H.A. Salim, H.E.M. Sallam, Efficient 3D modeling of damage in composite materials, J. Compos. Mater., 49(7) (2015) 817-828.

[25] M. Atta, A.A. Abd-Elhady, A. Abu-Sinna, H.E.M. Sallam, Prediction of failure stages for double lap joints using finite element analysis and artificial neural networks, Eng. Fail. Anal., 97 (2019) 242-257.

[26] A.A. Abd-Elhady, H.E.M. Sallam, Crack sensitivity of bolted metallic and polymeric joints, Eng. Fract. Mech., 147 (2015) 55-71.

[27] N. Aleksandrova, Engineering stress solutions for bolted and pressurized steel structures, Structures, 1 (2015) 60-66.

[28] A. Abu-Sinna, A.A. Abd-Elhady, M. Atta, H.E.M. Sallam, the failure stages of bolted double-lap metallic joints: an experimental study, J. Braz. Soc. Mech. Sci. Eng., 40(8) (2018) 388.

[29] A. Ataei, M.A. Bradford, X. Liu, Experimental study of flush end-plate beam-to-column composite joints with precast slabs and deconstructable bolted shear connectors, Structures, 7 (2016) 43-58.

[30] A. Anas, S. Guezouli, M. Couchaux, Component-based model versus stress-resultant plasticity modelling of bolted end-plate connection: numerical implementation, Structures, 11 (2017) 164-177.

[31] L. Zhao, M. Shan, F. Liu, J. Zhang, A probabilistic model for strength analysis of composite double-lap and single-bolt joints, Compos. Struct., 161 (2017) 419-427.

[32] J. Wang, J. Wang, H. Wang, Seismic behavior of blind bolted CFST frames with semi-rigid connections, Structures, 9 (2017) 91-104.

[33] N. Konkong, K. Phuvoravan, An analytical method for determining the load distribution of single-column multi bolt connection, Adv. Civ. Eng., 2017 (2017) 1912724.

[34] A.E.D. El-Sisi, H.E.D. Sallam, H.A. Salim, O.M. El-Husseiny, Structural behavior of hybrid CFRP/steel bolted staggered joints, Constr. Build. Mater., 190 (2018) 1192-1207.

[35] G.Tang, L. Yin, Z. Li, Y. Li, L. You, Structural behaviors of bolted connections using laminated bamboo and steel plates, Structures, 20 (2019) 324-339.

[36] A.A. Abd-Elhady, A. Abu-Sinna, M. Atta, H.E.M. Sallam, Identification of damage stages in bolted metallic joints for different joint geometries and tightening torque using statistical analysis, Adv. Struct. Eng., 23(5) (2020) 911-923.

[37] L. F. M. Da Silva, A. Ochsner, R.D. Adams, Handbook of Adhesion Technology, Springer, Berlin, Heidelberg (2011).

[38] ASTM D5961 / D5961M-05, Standard Test Method for Bearing Response of Polymer Matrix Composite Laminates, ASTM International, West Conshohocken, PA (2005).

[39] P.P. Camanho, S. Bowron, F.L. Matthews, Failure mechanisms in bolted CFRP, J. Reinf. Plast. Compos., 17(3) (1998) 205-233.

[40] U.A. Khashaba, H.E.M. Sallam, A.E. Al-Shorbagy, M.A. Seif, Effect of washer size and tightening Torque on the performance of bolted joints in composite structures, Compos. Struct., 73 (3) (2006) 310-317.

[41] B. Vangrimde, R. Boukhili, Bearing stiffness of glass fiber-reinforced polyester: influence of coupon geometry and laminate properties, Compos. Struct., 58(1) (2002) 57-73.

[42] A.A. Abd-Elhady, M.A. Mubaraki, H.E.M. Sallam, Progressive failure prediction of pinned joint in quasi-isotropic laminates used in pipelines, Lat. Am. J. Solids Struct., 15(6) (2018) e96.

[43] J. Hassan, T. Feser, R.M. O'Higgins, M. Waimer, C.T. McCarthy, N. Toso, M.E. Byrne, M.A. McCarthy, Energy absorption capability of composite bolted joints undergoing extended bearing failure, Compos. Struct., 237 (2020) 111868.

[44] B. Carcaterra, G. Ngaile, Investigation of energy storage in bolted joint components and the development of a geometry selection design tool for Belleville washers, Eng. Struct., 178 (2019) 436-443.